

RESEARCH

Open Access



Multiple amino acid substitutions involved in the adaptation of three avian-origin H7N9 influenza viruses in mice

Jianru Qin, Ouyang Peng, Xiaoting Shen, Lang Gong, Chunyi Xue* and Yongchang Cao*

Abstract

Background: Avian influenza A H7N9 virus has caused five outbreak waves of human infections in China since 2013 and posed a dual challenge to public health and poultry industry. The number of reported H7N9 virus human cases confirmed by laboratory has surpassed that of H5N1 virus. However, the mechanism for how H7N9 influenza virus overcomes host range barrier has not been clearly understood.

Methods: To generate mouse-adapted H7N9 influenza viruses, we passaged three avian-origin H7N9 viruses in mice by lung-to-lung passages independently. Then, the characteristics between the parental and mouse-adapted H7N9 viruses was compared in the following aspects, including virulence in mice, tropism of different tissues, replication in MDCK cells and molecular mutations.

Results: After ten passages in mice, MLD₅₀ of the H7N9 viruses reduced >750-3,160,000 folds, and virus titers in MDCK cells increased 10-200 folds at 48 hours post-inoculation. Moreover, the mouse-adapted H7N9 viruses showed more expanded tissue tropism and more serious lung pathological lesions in mice. Further analysis of the amino acids changes revealed 10 amino acid substitutions located in PB2 (E627K), PB1 (W215R and D638G), PA (T97I), HA (H3 numbering: R220G, L226S, G279R and G493R) and NA (P3Q and R134I) proteins. Moreover, PB2 E627K substitution was shared by the three mouse-adapted viruses (two viruses belong to YRD lineage and one virus belongs to PRD lineage), and PA T97A substitution was shared by two mouse-adapted viruses (belong to YRD lineage).

Conclusions: Our result indicated that the virulence in mice and virus titer in MDCK cells of H7N9 viruses significantly increased after adapted in mouse model. PB2 E627K and PA T97A substitutions are vital in mouse adaptation and should be monitored during epidemiological study of H7N9 virus.

Keywords: H7N9 influenza virus, virulence, adaptation, mouse, amino acid substitution

Background

A novel reassortant avian influenza H7N9 virus was first detected in February 2013 and since then, it has posed an unprecedented threat to both public health and poultry industry [1, 2]. Until September 5, 2018, H7N9 influenza virus has caused 1,567 human infections, and 615 deaths, with a fatality rate of approximately 39% (World Health Organization, WHO). The number of laboratory confirmed human infections with H7N9 virus has surpassed that of H5N1 virus [3]. The novel H7N9 virus including avian-origin virus has been reported to

be a tri-reassortant virus of H7, N9 and H9N2 influenza viruses [4, 5], and isolates from five epidemic waves of H7N9 influenza virus can be divided into many clades based on analysis of its genes [6–8]. However, numerous of new clades are continually occurring, indicated the continued evolution of H7N9 virus [9]. Moreover, highly pathogenic (HP) H7N9 virus were reported in late February 2017, which raised more concern about the pandemic threat of H7N9 virus [10, 11]. Herein, it is in urgent need to understand pathogenesis of H7N9 virus for control of this disease.

Though mouse is not a natural host of influenza viruses, it has been one of the most widely used animal models and has been applied to numerous areas of

* Correspondence: xuechy@mail.sysu.edu.cn; caoych@mail.sysu.edu.cn
State Key Laboratory of Biocontrol, School of Life Sciences, Higher Education Mega Center, Sun Yat-sen University, Guangzhou 510006, China



influenza research, including vaccine evaluation, virulence identification, virus adaptation, host-range comparison and so on [12–14]. Mice as an excellent animal model to study the mammalian adaptation of avian influenza viruses has been used for more than two decades [15–17]. A lot of previous work has convincingly proved that influenza virus could increase virulence in mice through lung-to-lung passage and many critical virulence-related sites were discovered by this method [18–20].

In this study, using sequential lung-to-lung passage in mice model, we adapted three H7N9 influenza viruses, A/Chicken/Guangdong/53/2014(H7N9) (H7N9-53), A/Chicken/Guangdong/MCX/2014(H7N9) (H7N9-MCX) and A/Chicken/Guangdong/ZSM/2017(H7N9) (H7N9-ZSM). Mouse-adapted H7N9 viruses were named H7N9-53 MA, H7N9-MCX MA and H7N9-ZSM MA, respectively. Evaluation of the virulence and replication feature of the six H7N9 viruses were conducted *in vivo* and *in vitro*. Moreover, sequencing and comparison of the whole genomes were performed to find out the amino acids that determine the increased virulence in the mouse.

Methods

Cells and viruses

Madin-Darby canine kidney (MDCK) cells were cultured in Dulbecco's Modified Eagle's Medium (DMEM, Gibco, NY) containing 10% fetal bovine serum (FBS, Gibco, NY) and used for assessment of H7N9 influenza virus replication.

A/Chicken/Guangdong/53/2014(H7N9) (H7N9-53), A/Chicken/Guangdong/MCX/2014(H7N9) (H7N9-MCX) and A/Chicken/Guangdong/ZSM/2017(H7N9) (H7N9-ZSM) were isolated from chickens in Guangdong, China and stored in our laboratory. H7N9-53 and H7N9-MCX belong to Yangtze River Delta (YRD) lineage and H7N9-ZSM belongs to Pearl River Delta (PRD) lineage.

Adaption of the three H7N9 influenza viruses in mice

The mouse-adapted H7N9 variants were derived from independent series of sequential lung-to-lung passages of viruses in mice as described previously [21]. In brief, fifteen 6-week-old female BALB/C mice were randomly divided into three groups of five mice and inoculated intranasally (i.n.) with 50 μ l of allantoic fluid containing the parental H7N9 viruses respectively. At 72 hours post-inoculation (hpi), lungs from the infected mice were harvested, homogenized and centrifuged. Supernatant was collected and inoculated to naïve mice at a volume of 50 μ l for the next passage. After a total of 10 passages in mice, the three H7N9 variants in final lung homogenate were amplified by 10-day-old SPF chicken eggs for 72 h at 37 °C to prepare virus stocks. Mouse-adapted H7N9 viruses were designated

as H7N9-53 MA, H7N9-MCX MA and H7N9-ZSM MA, respectively.

EID₅₀ and MLD₅₀

Groups of 4–6 10-day-old specific pathogen-free (SPF) chicken eggs were inoculated with a series of ten-fold dilutions of the H7N9 viruses or supernatants of the homogenized organ samples at the amount of 0.1 ml. At 72 hpi, hemagglutination (HA) assay was performed to test HA titers in allantoic fluids. HA titer $\geq 4 \log_2$ are defined as positive [22]. H7N9 viral titers in allantoic fluid and organ samples from infected mice were expressed as \log_{10} EID₅₀/ml. The detection limit of this assay was a titer of 0.75 \log_{10} EID₅₀/ml, and samples with titers less than 0.75 were assigned a value of 0.5.

The 50% mouse lethal dose (MLD₅₀) of the six H7N9 viruses was performed as previously described [23]. Briefly, groups of five 6-week-old female BALB/C mice were inoculated intranasally (i.n.) with a series of ten-fold dilutions of the H7N9 virus at the volume of 50 μ l, and mice inoculated with PBS was set as control. The mice were monitored daily for death for 14 days after inoculation and mouse that lost $\geq 25\%$ body weight was humanely euthanized and regarded as dead. The values of EID₅₀ and MLD₅₀ were calculated by Reed–Muench method.

Virulence comparison in mice

To compare the virulence of mouse-adapted H7N9 variants with parental H7N9 viruses *in vivo*, 6-week-old female BALB/C mice were inoculated intranasally (i.n.) with 10⁶ EID₅₀ of the six H7N9 influenza viruses in 50 μ l volume of PBS and monitored daily for weight loss and death for 14 days, respectively (n=5 per group). Moreover, mice inoculated with PBS was set as negative control. For determination of lung viral loads, three mice in each group were euthanized at 3 and 5 days post infection (dpi) and virus titers in lungs were determined by plaque assay. Furthermore, samples of hearts, liver, spleens, kidneys and brains were also collected at 3 dpi for determination of virus tissue tropism. Briefly, the organ samples were homogenized in 1 ml PBS and centrifuged at 10,000 \times rpm for 10 min at 4°C, and the supernatant was used for test of EID₅₀. Histopathological and immunohistochemistry (IHC) examination were also performed to identify lung lesions 3 dpi. In brief, lungs were fixed in neutral-buffered 10% formalin for 48 h, then embedded in paraffin. The paraffin-embedded lung tissues were sectioned at 4 μ m and stained with haematoxylin and eosin (H&E) for examination under a light microscopy. Examination of influenza viral antigen in the lungs was performed by immunohistochemical analysis using an anti-influenza nucleoprotein (NP) antibody as previous described [24].

Viral growth kinetics in MDCK cells

Viral growth kinetics in MDCK cells were used for comparison of mouse-adapted H7N9 variants and parental H7N9 viruses *in vitro*. MDCK cells were infected with H7N9 viruses at a multiplicity of infection (MOI) of 0.01, after incubation for one hour, MDCK cells were washed three times and overlaid with DMEM containing 1-2 $\mu\text{g/ml}$ TPCK-treated trypsin. Supernatant was collected at 12, 24, 36, 48, 60 and 72 hpi. Virus titration in MDCK cells was determined by plaque assay and calculated by Reed–Muench method. Titers of virus were expressed as \log_{10} PFU/ml.

Sequence analysis

Viral RNA of the six H7N9 influenza viruses was extracted from the allantoic fluids using Trizol Reagent and reversed into cDNA by reverse transcription. Eight influenza viral gene segments were amplified by PCR as previously described [25] and sequenced by GENEWIZ biotechnology Co. Ltd. The results of sequencing were aligned by Lasergene sequence analysis software package (DNASTar, Madison, WI). The GeneBank accession numbers corresponding to H7N9-53 virus are MH553113-MH553119 and KY221841; H7N9-MCX are MH553124-MH553130 and KY221844; H7N9-ZSM are MH553137-MH553144 (Additional file 1: Table S1).

Statistical analysis

Statistics analysis were performed using GraphPad Prism 6. Unpaired Student's t-tests or ANOVA followed by Dunnett's multiple comparison tests were used for statistical comparisons and statistics analysis. Statistical difference between two groups was indicated by * ($p < 0.05$), ** ($p < 0.01$), *** ($p < 0.001$) and **** ($p < 0.0001$).

Results

Adaption of H7N9 influenza viruses to mice

Firstly, the pathogenicity of parental H7N9-53, H7N9-MCX and H7N9-ZSM were evaluated in mice, and the three H7N9 viruses were unlethal to mice even at a high dose of $10^{8.0}$ EID₅₀ (Table 1). In order to generate mouse-adapted variants (designated as H7N9-53 MA, H7N9-MCX MA and H7N9-ZSM MA, respectively), serial lung-to-lung passages of the three H7N9 viruses were performed in mice independently. After 10 passages, MLD₅₀ of H7N9-53 MA, H7N9-MCX MA and H7N9-ZSM MA were 4.32, 5.12 and 1.50 \log_{10} EID₅₀/ml, respectively (Table 1). Compared to the parental H7N9 viruses, MLD₅₀ of the mouse-adapted variants decreased $10^{2.88}$ - $10^{6.50}$ folds. These results indicated that the virulence of the three H7N9 influenza viruses markedly increased in mice through serial passages.

Table 1. MLD₅₀ of the parental and mouse-adapted H7N9 viruses

Influenza virus	MLD ₅₀ (\log_{10} EID ₅₀ /ml)	Decrease in MLD ₅₀ (\log_{10} EID ₅₀ /ml)
H7N9-53	>8.0	-
H7N9-53 MA	4.32	>3.68
H7N9-MCX	>8.0	-
H7N9-MCX MA	5.12	>2.88
H7N9-ZSM	>8.0	-
H7N9-ZSM MA	1.50	>6.5

-: Not applicable

Pathogenicity feature and tissue tropism of H7N9 viruses in mice

To compare the virulence of the parental and mouse-adapted H7N9 viruses *in vivo*, mice were inoculated intranasally (i.n.) with 10^6 EID₅₀ of each virus and a series of assays including body changes, survival rates, virus titers in different tissues, histopathological and immunohistochemistry examination were carried out.

Mice infected with the parental H7N9 influenza virus survived 14 days with a slight weight loss, but they recovered to normal body weight soon (H7N9-ZSM recovered to normal body weight at 12 dpi, and mice inoculated with it were the latest recovered) (Fig. 1a, b). In contrast, mice infected with the mouse-adapted variants lost body weight from 2-3 dpi (Fig. 1a), and they showed severe post-infection symptoms, such as mental depression, severe emaciation, lumbar back arch, loss of appetite, ruffled fur and all succumbed to infection at 8 dpi (Fig. 1b).

Lung viral loads were determined 3 and 5 days after inoculation with each H7N9 viruses and the results showed lung viral titers of the mouse-adapted variants were significantly higher than that of their parental viruses no matter at 3 dpi ($p = 0.0061$ - 0.0491) or at 5 dpi ($p = 0.0007$ - 0.0360) (Fig. 2a). Moreover, Lung viral titers at 5 dpi were higher than at 3 dpi demonstrated constant replication of viruses in lungs (Fig. 2a). The lung viral titers of H7N9-53 vs H7N9-53 MA, H7N9-MCX vs H7N9-MCX MA, H7N9-ZSM vs H7N9-ZSM MA were 4.38 ± 0.39 vs 6.11 ± 0.24 , 3.02 ± 0.23 vs 4.01 ± 0.41 , 5.55 ± 0.21 vs 7.34 ± 0.60 at 3 dpi and 5.16 ± 0.24 vs 7.29 ± 0.21 , 5.39 ± 0.61 vs 7.1 ± 0.27 , 6.51 ± 0.11 vs 8.50 ± 0.90 at 5dpi. Taken together, the three mouse-adapted H7N9 variants replicated more effectively in mice lungs compared to their parental H7N9 viruses.

Furthermore, virus titers in heart, liver, spleen, lung, kidney and brain were tested for comparison of tissue tropism between the parental and mouse-adapted H7N9 viruses at 3 dpi. H7N9 mouse-adapted variants could be detected in all tissues, but H7N9 parental viruses could not be detected in any tissues except of lungs (Fig. 2b).

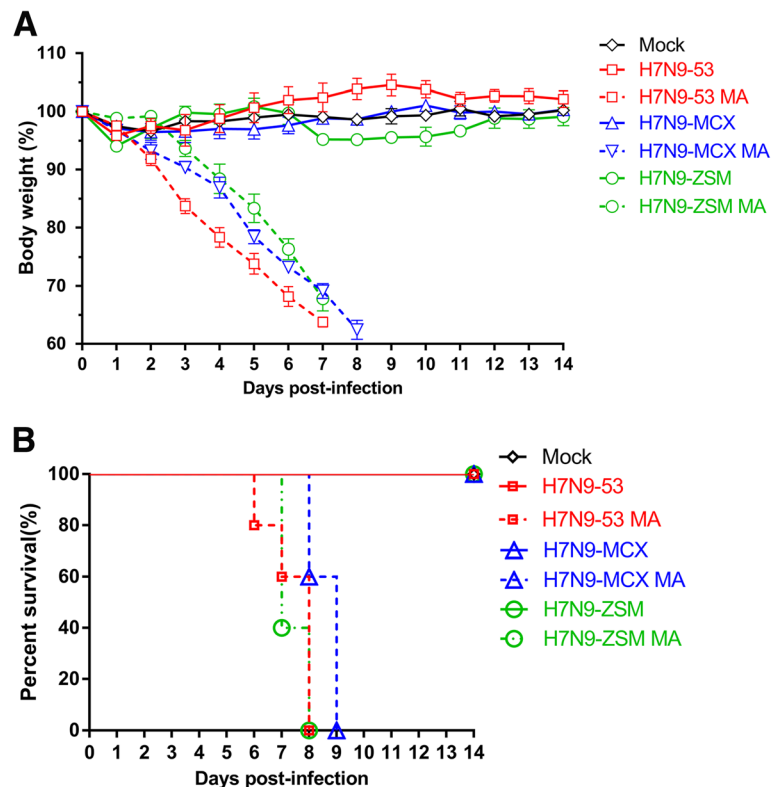


Fig. 1. Pathogenicity of the parental and mouse-adapted H7N9 viruses in mice. Groups of 5 6-week-old female BALB/C mice were inoculated i.n. with 10^6 EID₅₀ (50 μ l) of H7N9-53, H7N9-53 MA, H7N9-MCX, H7N9-MCX MA, H7N9-ZSM, H7N9-ZSM MA and PBS, respectively. Body weight changes and survival rates were monitored daily for 14 days. **a** Weight changes were recorded daily and represented by means (\pm standard deviation). **b** Mortality was determined by percentage of the surviving mice.

Virus titers in tissues from the mouse-adapted H7N9 variants revealed that lungs were the highest, followed by livers, hearts, brains, virus titers in spleens and kidneys were the lowest. All, H7N9-53 MA, H7N9-MCX MA and H7N9-ZSM MA had more expanded tissue tropism in mice than H7N9-53, H7N9-MCX and H7N9-ZSM (Fig. 2b).

Histopathological examination of lungs revealed that mice inoculated with the mouse-adapted H7N9 variants showed severe lesions with congestion, inflammatory cells infiltration or deciduous cells in the bronchial lumen. However, lesions in lungs from mice inoculated with the parental H7N9 viruses were relatively mild (Fig. 3a). Viral detection in lungs by IHC showed that positive stained cells were widely distributed in the mouse-adapted H7N9 variants groups, indicating lung viral loads were high. Positive signals were relatively weak in mice lungs from the parental H7N9 viruses (Fig. 3b). Neither lesion nor H7N9 virus antigen was observed in lungs from mock mice as expected (Fig. 3).

Growth characteristics of H7N9 viruses in MDCK cells

Comparison of replication ability *in vitro* between the parental and mouse-adapted H7N9 viruses was also

conducted in MDCK cells. Growth kinetics revealed that compared to their parental H7N9 viruses, the mouse-adapted H7N9 viruses grew faster and achieved to higher titers (Fig. 4). All the six H7N9 viruses reached the highest virus titers at 48 hpi, and the mean titers of H7N9-53, H7N9-53 MA, H7N9-MCX, H7N9-MCX MA, H7N9-ZSM and H7N9-ZSM MA were 5.52, 7.18, 3.52, 4.52, 7.55 and 9.89 log₁₀PFU/ml, respectively ($p=0.0078-0.0296$) (Fig. 4). These results indicated that the increased virulence in mice of the mouse-adapted viruses accompanied by the enhanced replication ability *in vitro*.

Sequence analysis

To further explore the molecular changes of mouse-adapted H7N9 viruses which increase the virulence in mice, genomes of the six H7N9 viruses were sequenced. The results revealed that there was a total of 13 amino acid differences located in 10 sites of influenza virus genomes between the parental and mouse-adapted H7N9 viruses, of which 5 between H7N9-53 and H7N9-53 MA, 5 between H7N9-MCX and H7N9-MCX MA, 3 between H7N9-ZSM and H7N9-ZSM MA, respectively. Moreover, E627K substitution in PB2 protein was the common substitution of the

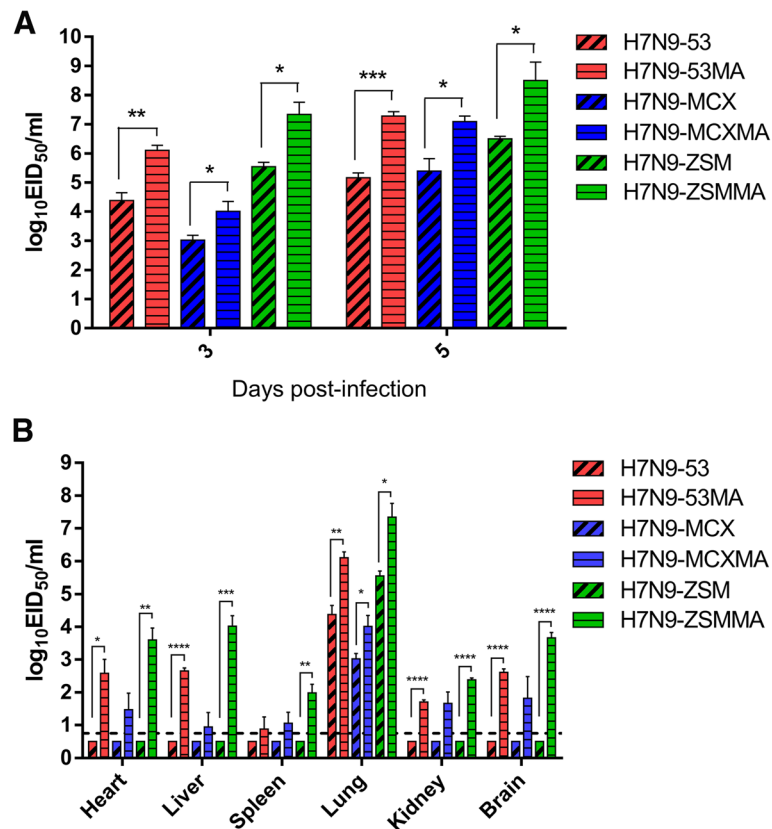


Fig. 2. Titers of virus in different tissues of the parental and mouse-adapted H7N9 viruses in mice. Groups of 6 6-week-old female BALB/C mice were inoculated i.n. with 10^6 EID₅₀ (50 μ l) of H7N9-53, H7N9-53 MA, H7N9-MCX, H7N9-MCX MA, H7N9-ZSM, H7N9-ZSM MA and PBS, respectively. 3 dpi, 3 mice were euthanized to collect hearts, liver, spleens, lungs, kidneys and brains for determination of virus titers by EID₅₀. The remaining 3 mice were euthanized for lung viral loads by 5 dpi. **a** Lung viral loads of mice inoculated with H7N9 virus at 3 and 5 dpi. **b** Viral distribution of H7N9 virus in different tissues. The limit of virus detection is indicated by a dotted line.

three mouse-adapted H7N9 viruses and PA T97I substitution was shared by H7N9-53 MA H7N9-ZSM MA. The amino acid substitutions were mapped in PB2, PB1, PA, HA and NA proteins (Table 2), and genes of NP, M and NS were 100% homologous.

In addition, we queried H7N9 sequences deposited in the GISAID EpiFlu database, and the number of H7N9 viruses with amino acid substitutions identified in this study were also displayed in the Table 3.

Discussion

Human infections of H7N9 virus have spread from mainland China to Hong Kong and Taiwan, even to Canada and Malaysia, causing unprecedented losses to public health (WHO). Though H7N9 virus does not possess sufficient ability for human-to-human transmission, it could effectively replicate in alveolar epithelial cells of mammals and transmit via respiratory droplets to kill ferrets [14], so it is hard to predict whether this disease will cause a pandemic in the future. H7N9 virus has generated multiple genotypes for continuous evolution [26].

In general, most of the isolates can be clustered to two lineages (YRD lineage and PRD lineage). YRD lineage includes Zhejiang, Jiangsu, Shanghai, and PRD lineage refers to Guangdong, Guangxi, Fujian, Hongkong [27]. Viruses of the YRD lineage reacted poorly with ferret antiserum raised by the PRD candidate vaccine (WHO). Herein, it is important to monitor the prevalence of H7N9 virus belonging to both YRD and PRD lineage. In this report, H7N9-53 and H7N9-MCX belong to YRD lineage, and H7N9-ZSM belongs to PRD lineage. Through adaptation in mice of the three H7N9 influenza viruses, we tried to seek virulence-associated mutations, as well as compare mouse-adapted substitutions between YPD and PRD lineages.

There are many factors influencing mammalian adaptation of avian influenza virus and the most important determinant is receptor-binding specificity [28]. As is known to all, the first step of influenza virus infection of host cells is binding to sialyloligosaccharides on the cell surface via hemagglutinin (HA) protein [29]. Avian influenza virus HAs prefer binding to α 2,3-linked sialic acids, whereas

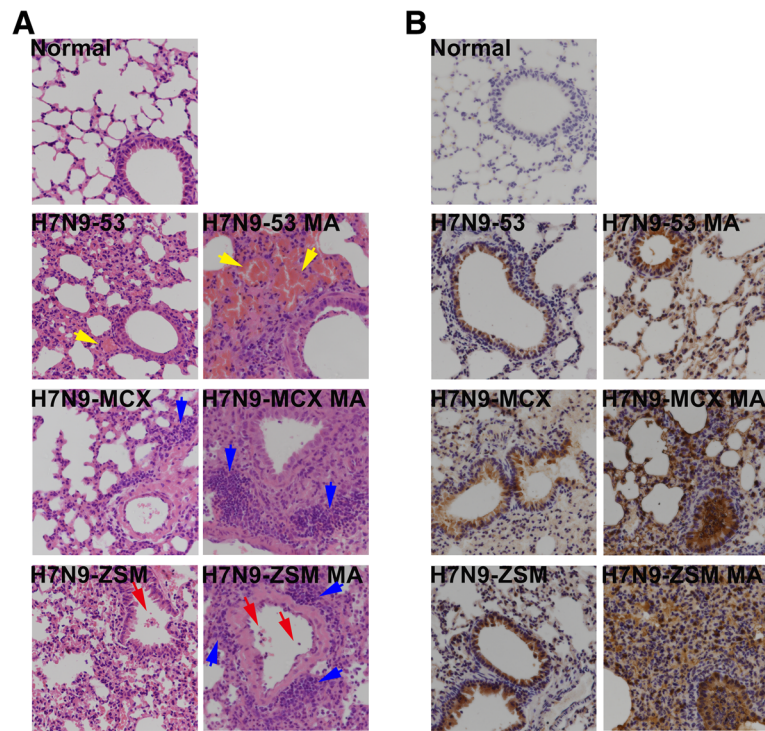


Fig. 3. Histopathology and immunohistochemistry examination of lungs of the parental and mouse-adapted H7N9 viruses. 3 days after the inoculation, the lungs ($n = 3$) were examined by H&E staining for pathological changes and by anti-influenza nucleoprotein (NP) antibody for detection of antigens ($\times 400$). **a** Histopathology examination. Yellow, blue and red arrows indicated congestion, inflammatory cells infiltration and deciduous cells in the bronchial lumen, respectively. **b** Immunohistochemistry examination.

HAs of human influenza virus prefer $\alpha 2,6$ -linked sialic acids [30]. Different sialic acid receptor-binding properties make host-range and change may result in crossing of host barrier [31]. Another major determinant of host-range is polymerase activity. Compared with temperature of mammalian upper respiratory tract, temperature of avian gastrointestinal tract is much higher (38°C of avian vs 33°C of

mammalian). Amino acid substitutions in polymerase protein usually lead to changing of viral replication efficiency in different respiratory tract [32, 33]. Moreover, N-linked glycosylation of HA protein is also an important factor influence on host-range of influenza virus. Glycosylation plays an important role in HA protein folding and HA antigenicity, and changes at glycosylation sites possible produce

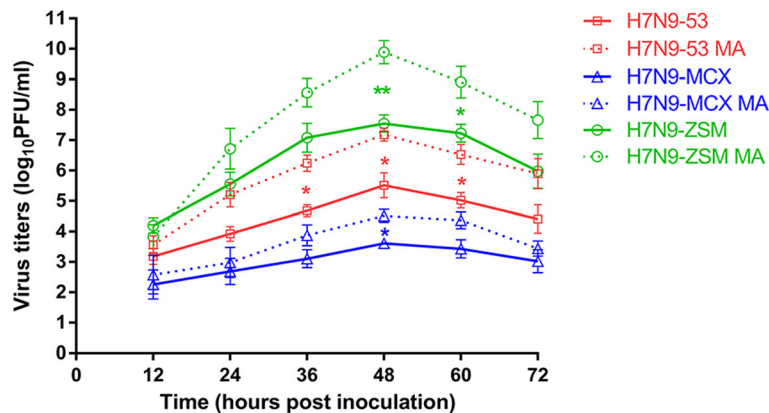


Fig. 4. Growth kinetics of the parental and mouse-adapted H7N9 viruses. MDCK cells were inoculated with H7N9-53, H7N9-53 MA, H7N9-MCX, H7N9-MCX MA, H7N9-ZSM, H7N9-ZSM MA (MOI=0.01), respectively. Supernatants of the cultured cells were collected at a 12-hour interval till 72 hpi. Subsequently, the virus titers were measured by plaque assay and represented by means (\pm standard deviation).

Table 2. Amino acid differences between the parental and mouse-adapted H7N9 viruses

Influenza virus	PB2	PB1	PA	HA		NP	NA	M	NS
	627	-	97	235 ^a (226 ^b)	288 ^a (279 ^b)	-	134	-	-
H7N9-53	E	-	T	L	G	-	R	-	-
H7N9-53 MA	K	-	I	S	R	-	I	-	-
	627	215	97	229 ^a (220 ^b)		-	3	-	-
H7N9-MCX	E	W	T	R		-	P	-	-
H7N9-MCX MA	K	R	I	G		-	Q	-	-
	627	638	-	503 ^a (493 ^b)		-	-	-	-
H7N9-ZSM	E	D	-	G		-	-	-	-
H7N9-ZSM MA	K	G	-	R		-	-	-	-

-: Not applicable

^a: H7 numbering^b: H3 numbering

improperly folded HA proteins and then affect the antigenicity of HA [34]. In addition to the above-mentioned factors, several determinants also contribute to mammal adaption, such as morphology of influenza virus, acid stability of HA protein and functional balance between HA and NA [35]. In this study, a total of 9 amino differences was discovered between the parental and mouse-adapted H7N9 viruses. Among the substitutions, 4 located in HA proteins, 2 in NA protein and 4 in polymerase proteins (1 in PB2, 2 in PB1 and 1 in PA protein).

Further comparison of the amino acids substitutions discovered that only E627K at PB2 protein shared by the three mouse-adapted H7N9 viruses. PB2 subunit has multiple domains and 627-nuclear localization signal (NLS) domain is the main region that involved in interaction with NP protein [36]. Moreover, PB2 627-NLS domain has been proved to play the role in transcription and replication of influenza virus RNA genome [37]. Many subtypes of influenza virus, including H3N2, H5N1, H5N5, H5N6, H6N1, H6N6, H7N1, H7N7,

Table 3. Count the number of H7N9 viruses with amino acid substitutions identified in this study

Segment	Position	Amino acid	Frequency of substitution (no. of strains with the substitution/total no. of strains)
PB2	627	E	1351/2370
		K	915/2370
PB1	215	W	1/2358
		R	2007/2358
		D	2197/2358
	638	G	41/2358
		T	2342/2357
PA	97	I	7/2357
		R	2619/2647
HA	229	G	1/2647
		L	2590/2647
	235	S	10/2647
		G	2276/2647
		R	7/2647
	288	G	12/2647
		R	0/2647
NA	503	P	2586/2620
		Q	1/2620
	3	R	2337/2620
		I	0/2620
		134	I

H7N9 and H9N2 have been reported increasing virulence by substitution of E627K at PB2 protein [38–40]. Moreover, the evaluation of H7N9 viruses isolated from avian species between 2013 and 2017 in China revealed some H7N9 viruses have readily obtained the 627K mutation in its PB2 segment upon replication in ferrets, causing it to become highly lethal in mice and ferrets [5]. In addition to the most often-observed substitution of E627K, there are several other important mutations in the PB2 protein, such as E158G, D253N, T271A, K526R, Q591K, A588V, D701N and so on, and these mutations had been proved to enhance polymerase activity [5, 16, 19, 20, 32]. Another substitution worth noting is T97I at PA protein. This substitution is shared by the two H7N9 viruses belonging to PRD lineage. PA T97I substitution was reported in mouse adaption of H5N2, H6N1, H7N1, H10N7 and H7N9 subtypes of influenza viruses [13, 41–47]. But much work needs to be done about the validation and mechanism. In addition, other substitutions discovered in this study have not been reported, indicating that these mutations are a specific selection of H7N9 virus.

One thing needs to be noted is that though 10 successive passages in mice were performed to obtain three mouse-adapted H7N9 influenza viruses, the pathogenicity to mice and replication in cells of the three mouse-adapted H7N9 viruses were different. The MLD₅₀ of H7N9-ZSM MA is 660 and 4,164 times less than that of H7N9-53 MA and H7N9-MCX MA, respectively. Virus titer in MDCK of H7N9-ZSMMA was the highest, followed by H7N9-53 MA, H7N9-MCX MA was the lowest. All these findings demonstrated that though E627K substitution is the common mutation of the three mouse-adapted viruses and it has been proved to increase virulence in mice, it is not the only virulence-determination mutation, there must be other substitutions correlate with E627K to influence virulence of mouse-adapted H7N9 virus.

Conclusion

The virulence and replicative ability of three H7N9 influenza viruses increased through the sequential lung-to-lung passages, and several mutations were found, which may influence on the virulence and growth characteristics of H7N9 viruses. Moreover, PB2 E627K and PA T97I may play important roles in H7N9 mammal adaption, but the exact role and other substitutions need further verification. Our study attaches great importance to the epidemiological surveillance of H7N9 virus.

Additional files

Additional file 1: Table S1. GeneBank accession numbers corresponding to the three H7N9 viruses. (DOCX 15 kb)

Abbreviations

WHO: World Health Organization; HP: Highly Pathogenic; MDCK: Madin-Darby canine kidney; DMEM: Dulbecco's Modified Eagle's Medium; FBS: Fetal bovine serum; H7N9-53: A/Chicken/Guangdong/53/2014(H7N9); H7N9-MCX: A/Chicken/Guangdong/MCX/2014(H7N9); H7N9-ZSM: A/Chicken/Guangdong/ZSM/2017(H7N9); YRD: Yangtze River Delta; PRD: Pearl River Delta; SPF: Specific pathogen-free; HA: Hemagglutinin; EID₅₀: 50% egg infectious dose; MLD₅₀: 50% mouse lethal dose; i.n.: Inoculated intranasally; dpi: days post infection; IHC: Immunohistochemistry; H&E: Haematoxylin and eosin; NP: Nucleoprotein; MOI: Multiplicity of infection; hpi: Hours post inoculation.

Acknowledgments

Not applicable

Funding

This work was supported by Guangdong Science and Technology Plan [grant number 2013B020224003], Guangdong Natural Science Foundation [grant number 2015A030313095] and H7N9 Avian Influenza Joint Research [grant number 2014-1046].

Availability of data and materials

Please contact author for data requests.

Authors' contributions

YC, CX and JQ conceived and designed the study; JQ, OP, XS and LG performed the experiments; JQ analyzed the data and wrote the original draft; All authors read and approved the final manuscript.

Ethics approval and consent to participate

The animal study was supervised by the Institutional Animal Care and Use Committee of the Sun Yat-sen University and performed in accordance with the regulation and guidelines of this committee (Permit number: SYSU-IACUC-2018-000109).

Consent for publication

All authors consent for publication.

Competing interests

The authors declare that they have no competing interests.

Publisher's Note

Springer Nature remains neutral with regard to jurisdictional claims in published maps and institutional affiliations.

Received: 22 August 2018 Accepted: 17 December 2018

Published online: 08 January 2019

References

- Gao R, Cao B, Hu Y, Feng Z, Wang D, Hu W, Chen J, Jie Z, Qiu H, Xu K, et al. Human infection with a novel avian-origin influenza A (H7N9) virus. *N Engl J Med*. 2013;368:1888–97.
- Yang H, Carney PJ, Chang JC, Guo Z, Stevens J. Structural and Molecular Characterization of the Hemagglutinin from the Fifth Epidemic Wave A(H7N9) Influenza Viruses. *J Virol*. 2018;92:e00375–18.
- Webby RJ, Yang Z. The changing landscape of A H7N9 influenza virus infections in China. *Lancet Infect Dis*. 2017;17:783–4.
- Wang N, Sun M, Wang W, Ouyang G, Chen Z, Zhang Y, Zhao B, Wu S, Huang J, Sun H, et al. Avian Influenza (H7N9) Viruses Co-circulating among Chickens, Southern China. *Emerg Infect Dis*. 2017;23:2100–2.
- Shi J, Deng G, Kong H, Gu C, Ma S, Yin X, Zeng X, Cui P, Chen Y, Yang H, et al. H7N9 virulent mutants detected in chickens in China pose an increased threat to humans. *Cell Res*. 2017;27:1409–21.
- Liu D, Shi W, Shi Y, Wang D, Xiao H, Li W, Bi Y, Wu Y, Li X, Yan J, et al. Origin and diversity of novel avian influenza A H7N9 viruses causing human infection: phylogenetic, structural, and coalescent analyses. *Lancet*. 2013;381:1926–32.
- Lam TT, Wang J, Shen Y, Zhou B, Duan L, Cheung CL, Ma C, Lycett SJ, Leung CY, Chen X, et al. The genesis and source of the H7N9 influenza viruses causing human infections in China. *Nature*. 2013;502:241–4.

8. Su S, Gu M, Liu D, Cui J, Gao GF, Zhou J, Liu X. Epidemiology, Evolution, and Pathogenesis of H7N9 Influenza Viruses in Five Epidemic Waves since 2013 in China. *Trends Microbiol.* 2017;25:713–28.
9. Shi J, Deng G, Ma S, Zeng X, Yin X, Li M, Zhang B, Cui P, Chen Y, Yang H, et al. Rapid Evolution of H7N9 Highly Pathogenic Viruses that Emerged in China in 2017. *Cell Host Microbe.* 2018;24:558–68.
10. Ke C, Mok C, Zhu W, Zhou H, He J, Guan W, Wu J, Song W, Wang D, Liu J, et al. Human Infection with Highly Pathogenic Avian Influenza A(H7N9) Virus, China. *Emerg Infect Dis.* 2017;23:1332–40.
11. Zhang F, Bi Y, Wang J, Wong G, Shi W, Hu F, Yang Y, Yang L, Deng X, Jiang S, et al. Human infections with recently-emerging highly pathogenic H7N9 avian influenza virus in China. *J Infect.* 2017;75:71–5.
12. Wang Y, Wu J, Xue C, Wu Z, Lin Y, Wei Y, Wei X, Qin J, Zhang Y, Wen Z, et al. A recombinant H7N9 influenza vaccine with the H7 hemagglutinin transmembrane domain replaced by the H3 domain induces increased cross-reactive antibodies and improved interclade protection in mice. *Antiviral Res.* 2017;143:97–105.
13. Wu H, Peng X, Peng X, Cheng L, Jin C, Lu X, Xie T, Yao H, Wu N. Multiple amino acid substitutions involved in the adaptation of avian-origin influenza A (H10N7) virus in mice. *Arch Virol.* 2016;161:977–80.
14. Imai M, Watanabe T, Kiso M, Nakajima N, Yamayoshi S, Iwatsuki-Horimoto K, Hatta M, Yamada S, Ito M, Sakai-Tagawa Y, et al. A Highly Pathogenic Avian H7N9 Influenza Virus Isolated from a Human Is Lethal in Some Ferrets Infected via Respiratory Droplets. *Cell Host Microbe.* 2017;22:615–26.
15. Terrence M, Tumpey D. Characterization of a Highly Pathogenic H5N1 Avian Influenza A Virus Isolated from Duck Meat. *J Virol.* 2002;12:6344–55.
16. Brown EG, Liu H, Kit LC, Baird S, Nesrallah M. Pattern of mutation in the genome of influenza A virus on adaptation to increased virulence in the mouse lung: Identification of functional themes. *P Natl Acad Sci USA.* 2001;98:6883–8.
17. Brown EG, Bailly JE. Genetic analysis of mouse-adapted influenza A virus identifies roles for the NA, PB1, and PB2 genes in virulence. *Virus Res.* 1999;61:63–76.
18. Yu Z, Cheng K, Sun W, Zhang X, Xia X, Gao Y. Multiple adaptive amino acid substitutions increase the virulence of a wild waterfowl-origin reassortant H5N8 avian influenza virus in mice. *Virus Res.* 2018;244:13–20.
19. Yu Z, Sun W, Zhang X, Cheng K, Zhao C, Gao Y, Xia X. Multiple amino acid substitutions involved in the virulence enhancement of an H3N2 avian influenza A virus isolated from wild waterfowl in mice. *Vet Microbiol.* 2017;207:36–43.
20. Manz B, Schwemmler M, Brunotte L. Adaptation of avian influenza A virus polymerase in mammals to overcome the host species barrier. *J Virol.* 2013;87:7200–9.
21. Zhang X, Xu G, Wang C, Jiang M, Gao W, Wang M, Sun H, Sun Y, Chang KC, Liu J, Pu J. Enhanced pathogenicity and neurotropism of mouse-adapted H10N7 influenza virus are mediated by novel PB2 and NA mutations. *J Gen Virol.* 2017;98:1185–95.
22. OIE (World Organization for Animal Health), 2014b. Manual of Diagnostic Tests and Vaccines for Terrestrial Animals 2018, chapter 2.3.4 Al. <http://www.oie.int/standard-setting/terrestrial-manual/access-online/>.
23. Yu Z, Sun W, Li X, Chen Q, Chai H, Gao X, Guo J, Zhang K, Wang T, Feng N, et al. Adaptive amino acid substitutions enhance the virulence of a reassortant H7N1 avian influenza virus isolated from wild waterfowl in mice. *Virology.* 2015;476:233–9.
24. Huo C, Zhang S, Zhang S, Wang M, Qi P, Xiao J, Hu Y, Dong H. Mice with type 1 diabetes exhibit increased susceptibility to influenza A virus. *Microb Pathog.* 2017;113:233–41.
25. Hoffmann E, Stech J, Guan Y, Webster RG, Perez DR. Universal primer set for the full-length amplification of all influenza A viruses. *Arch Virol.* 2001;146:2275–89.
26. Ding X, Luo J, Quan L, Wu A, Jiang T. Evolutionary genotypes of influenza A (H7N9) viruses over five epidemic waves in China. *Infect Genet Evol.* 2017;55:269–76.
27. Xiang D, Pu Z, Luo T, Guo F, Li X, Shen X, Irwin DM, Murphy RW, Liao M, Shen Y. Evolutionary dynamics of avian influenza A H7N9 virus across five waves in mainland China, 2013–2017. *J Infect.* 2018.
28. Imai M, Kawaoka Y. The role of receptor binding specificity in interspecies transmission of influenza viruses. *Curr Opin Virol.* 2012;2:160–7.
29. Zhao H, Zhou J, Jiang S, Zheng BJ. Receptor binding and transmission studies of H5N1 influenza virus in mammals. *Emerg Microbes Infect.* 2013;2:e85.
30. Shinya K, Ebina M, Yamada S, Ono M, Kasai N, Kawaoka Y. Avian flu: influenza virus receptors in the human airway. *Nature.* 2006;440:435–6.
31. Tumpey TM, Maines TR, Van Hoeven N, Glaser L, Solorzano A, Pappas C, Cox NJ, Swayne DE, Palese P, Katz JM, Garcia-Sastre A. A two-amino acid change in the hemagglutinin of the 1918 influenza virus abolishes transmission. *Science.* 2007;315:655–9.
32. Taft AS, Ozawa M, Fitch A, Depasse JV, Halfmann PJ, Hill-Batorski L, Hatta M, Friedrich TC, Lopes TJ, Maher EA, et al. Identification of mammalian-adapting mutations in the polymerase complex of an avian H5N1 influenza virus. *Nat Commun.* 2015;6:7491.
33. Li W, Lee H, Li RF, Zhu HM, Yi G, Peiris J, Yang ZF, Mok C. The PB2 mutation with lysine at 627 enhances the pathogenicity of avian influenza (H7N9) virus which belongs to a non-zoonotic lineage. *Sci Rep.* 2017;7:2352.
34. Sun X, Jayaraman A, Mani Prasad P, Raman R, Houser KV, Pappas C, Zeng H, Sasisekharan R, Katz JM, Tumpey TM. N-linked glycosylation of the hemagglutinin protein influences virulence and antigenicity of the 1918 pandemic and seasonal H1N1 influenza A viruses. *J Virol.* 2013;87:8756–66.
35. Cauldwell AV, Long JS, Moncorge O, Barclay WS. Viral determinants of influenza A virus host range. *J Gen Virol.* 2014;95:1193–210.
36. Hsia HP, Yang YH, Szeto WC, Nilsson BE, Lo CY, Ng AK, Fodor E, Shaw PC. Amino acid substitutions affecting aspartic acid 605 and valine 606 decrease the interaction strength between the influenza virus RNA polymerase PB2 '627' domain and the viral nucleoprotein. *Plos One.* 2018;13:e191226.
37. Nilsson BE, Te VA, Fodor E. Role of the PB2 627 Domain in Influenza A Virus Polymerase Function. *J Virol.* 2017;91:e02467-16.
38. Chen Q, Yu Z, Sun W, Li X, Chai H, Gao X, Guo J, Zhang K, Feng N, Zheng X, et al. Adaptive amino acid substitutions enhance the virulence of an H7N7 avian influenza virus isolated from wild waterfowl in mice. *Vet Microbiol.* 2015;177:18–24.
39. Peng X, Liu F, Wu H, Peng X, Xu Y, Wang L, Chen B, Sun T, Yang F, Ji S, Wu N. Amino Acid Substitutions HA A150V, PA A343T, and PB2 E627K Increase the Virulence of H5N6 Influenza Virus in Mice. *Front Microbiol.* 2018;9:453.
40. Zhang C, Zhao Z, Guo Z, Zhang J, Li J, Yang Y, Lu S, Wang Z, Zhi M, Fu Y, et al. Amino Acid Substitutions Associated with Avian H5N6 Influenza A Virus Adaptation to Mice. *Front Microbiol.* 2017;8:1763.
41. Cheng K, Yu Z, Chai H, Sun W, Xin Y, Zhang Q, Huang J, Zhang K, Li X, Yang S, et al. PB2-E627K and PA-T97I substitutions enhance polymerase activity and confer a virulent phenotype to an H6N1 avian influenza virus in mice. *Virology.* 2014;468-470:207–13.
42. Nam JH, Shim SM, Song EJ, Espano E, Jeong DG, Song D, Kim JK. Rapid virulence shift of an H5N2 avian influenza virus during a single passage in mice. *Arch Virol.* 2017;162:3017–24.
43. Zhao Y, Yu Z, Liu L, Wang T, Sun W, Wang C, Xia Z, Gao Y, Zhou B, Qian J, Xia X. Adaptive amino acid substitutions enhance the virulence of a novel human H7N9 influenza virus in mice. *Vet Microbiol.* 2016;187:8–14.
44. Yu Z, Cheng K, Xin Y, Sun W, Li X, Huang J, Zhang K, Yang S, Wang T, Zheng X, et al. Multiple amino acid substitutions involved in the adaptation of H6N1 avian influenza virus in mice. *Vet Microbiol.* 2014;174:316–21.
45. Nam JH, Kim EH, Song D, Choi YK, Kim JK, Poo H. Emergence of Mammalian Species-Infectious and -Pathogenic Avian Influenza H6N5 Virus with No Evidence of Adaptation. *J Virol.* 2011;85:13271–7.
46. Song MS, Pascua PNQ, Lee JH, Baek YH, Lee OJ, Kim CJ, Kim H, Webby RJ, Webster RG, Choi YK. The Polymerase Acidic Protein Gene of Influenza A Virus Contributes to Pathogenicity in a Mouse Model. *J Virol.* 2009;83:12325–35.
47. Rigoni M, Shinya K, Toffan A, Milani A, Bettini F, Kawaoka Y, Cattoli G, Capua I. Pneumo- and neurotropism of avian origin Italian highly pathogenic avian influenza H7N1 isolates in experimentally infected mice. *Virology.* 2007;364:28–35.